Mixed convection boundary layer flow of a viscoelastic fluid over a horizontal circular cylinder

Ilyana Anwar, Norsarahaida Amin, Ioan Pop

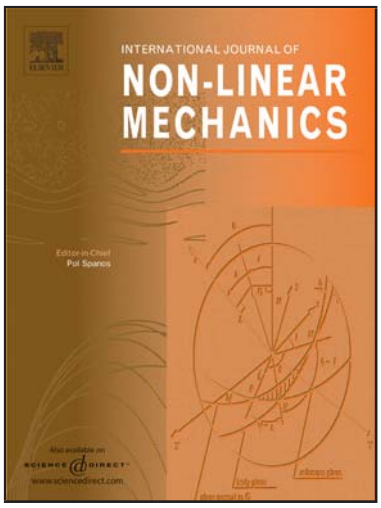

www.elsevier.com/locate/nlm

Mixed convection boundary layer flow of a viscoelastic fluid over a horizontal circular cylinder

Ilyana Anwar, Norsarahaida Amin, Ioan Pop

PII: S0020-7462(08)00092-9
DOI: doi:10.1016/j.ijnonlinmec.2008.04.008
Reference: NLM 1478

To appear in: *International Journal of Non-Linear Mechanics*

Received date: 18 January 2008
Revised date: 21 April 2008
Accepted date: 22 April 2008

Cite this article as: Ilyana Anwar, Norsarahaida Amin and Ioan Pop, Mixed convection boundary layer flow of a viscoelastic fluid over a horizontal circular cylinder, *International Journal of Non-Linear Mechanics* (2008), doi:10.1016/j.ijnonlinmec.2008.04.008

Mixed convection boundary layer flow of a viscoelastic fluid over a horizontal circular cylinder

Ilyana Anwar and Norsarahaida Amin

Department of Mathematics, Universiti Teknologi Malaysia,
Johor Bahru, Johor, Malaysia

Ioan Pop*

Faculty of Mathematics, University of Cluj, R-3400 Cluj, Romania

Abstract

The steady mixed convection boundary layer flow of a viscoelastic fluid over a horizontal circular cylinder in a stream flowing vertically upwards is numerically studied for both cases of heated and cooled cylinders. The governing partial differential equations are transformed into dimensionless forms using an appropriate transformation and then solved numerically using the Keller-box method. The comparison between the solutions obtained and those for a Newtonian fluid is found to be very good. Effects of the mixed convection and elasticity parameters on the skin friction and heat transfer coefficients for a fluid having the Prandtl number equal to one are also discussed. It is found that for some values of the viscoelastic parameter and some negative values of the mixed convection parameter (opposing flow) the boundary layer separates from the cylinder. Heating the cylinder delays separation and can, if the cylinder is warm enough, suppress the separation completely. Similar to the case of a Newtonian fluid, cooling the cylinder brings the separation point nearer to the lower stagnation point. However, for a sufficiently cold cylinder there will not be a boundary layer.

Keywords: Viscoelastic fluid; Boundary layer; Mixed convection; Circular cylinder; Numerical method

1. Introduction

There are many fluids whose behaviour cannot be described by the classical Navier-Stokes and boundary layer equations. The homogeneous and incompressible second grade fluid is one of the many models that have been proposed to describe the non-Newtonian behaviour of such fluids (see Kumari et al. [1]). Mechanics of non-linear fluids present a special challenge to researchers due to its many

* Corresponding author.

E-mail address: pop.ioan@yahoo.co.uk (I. Pop)

practical applications, for example, in the design of thrust bearings and radial diffusers, drag reduction, transpiration cooling and thermal oil recovery, to mention just a few. One of the simplest ways in which the viscoelastic fluids have been classified is the methodology proposed by Rivlin and Ericksen [2] and Truesdell and Noll [3], who presented constitutive relations for the stress tensor $\mathbf{T}$ as a function of the symmetric part of the velocity gradient $\mathbf{D}$, and its higher (total) derivatives (see Massoudi [4]). The boundary layer theory for second-grade fluids has been developed by Oldroyd [5], Beard and Walters [6] and Rajagopal et al. [7]. However, the boundary layer equations are an order higher than those for the Newtonian (viscous) fluid and the adherence boundary conditions are insufficient to determine the solution of these equations completely. Therefore, we need a boundary condition in addition to the usual adherence boundary conditions. Rajagopal [8,9] and Rajagopal and Kaloni [10] have discussed this question in detail. Garg and Rajagopal [11,12] studied the flow of a fluid of second grade near the stagnation point of a semi-infinite wall by augmenting the boundary condition at infinity. It has been shown that their results agree well with the results of Rajeswari and Rathna [13] based on the series expansion for small values of the viscoelastic parameter ε, which multiplies the highest-order spatial derivative in their equation. The advantage of augmenting the boundary conditions over the perturbation approach is that the analysis is valid even for large values of the parameter ε and, as shown by Garg and Rajagopal [11], significant deviations from the Newtonian behaviour are possible for even moderately large values of ε. The augmenting of the boundary condition at infinity has also been used by Kumari et al. [1] for the steady non-similar mixed convection boundary layer flow of a viscoelastic fluid over a permeable vertical wedge, by Ariel [14] for the two-dimensional stagnation point flow of a second grade fluid, by Garg [15] for the flow of an incompressible fluid of second grade past a wedge with suction at the surface and by Cortell [16] for the flow and heat transfer of a second grade fluid past a stretching sheet. Very recently, Hayat and Sajid [17] presented an analytic solution using the homotopy analysis method (HAM) for the flow and heat transfer of a second grade fluid over a radially stretching sheet. Also, Mushtaq et al. [18] studied the effects of thermal buoyancy on flow of a second grade fluid along a vertical, continuous stretching sheet of which the velocity and temperature distributions are assumed to vary according to a power-law form. The governing partial differential equations are non-similar and they were solved using (1) the series expansion method together with the Shanks transformation, (2) the local non-similarity method with second level of truncation and (3) the Keller-box method for some values of the mixed convection parameter. However, the authors have not mentioned whether they have used the extra boundary condition at infinity or not.

In this paper, the steady non-similar mixed convection boundary layer flow of a viscoelastic fluid over a horizontal circular cylinder is considered. The coupled nonlinear partial differential equations

governing the flow have been solved numerically using a very efficient finite-difference scheme, known as the Keller-box method, which is described in the book by Cebeci and Bradshaw [19] after augmenting the boundary condition at infinity. The effects of the mixed convection and viscoelastic parameters on the skin friction and heat transfer around the cylinder are studied. The effects of these parameters on the velocity and temperature profiles near the lower stagnation point of the cylinder are presented here only for the Prandtl number equal to one, although they can be obtained for other values of the Prandtl number, as well. The particular cases of the present results for a viscous (Newtonian) fluid have been compared with those of Merkin [20] and Nazar *et al*. [21]. The results have also been compared with those of Hiemenz [22] and Eckert [23] for a viscous fluid and with those of Ariel [14] for a viscoelastic fluid when the buoyancy forces are absent. It is shown that the agreement between all these results is very good. We wish also to mention to this end that to our best knowledge this classical very important problem has not been studied before for a viscoelastic fluid so that the results are new for these fluids.

2. Basic equations

The problem that we will study in this paper is the steady mixed convection boundary layer flow past an isothermal horizontal circular cylinder of radius a placed in a viscoelastic fluid. Figure 1 illustrates the geometry of the problem and the corresponding coordinate system. It is assumed that the constant temperature of the surface of the cylinder is T_w, and that of the ambient fluid is T_∞, where $T_w > T_\infty$ corresponds to a heated cylinder (assisting flow) and $T_w < T_\infty$ corresponds to a cooled cylinder (opposing flow), respectively. It is also assumes that the viscous dissipation is neglected. Further, following Merkin [20],

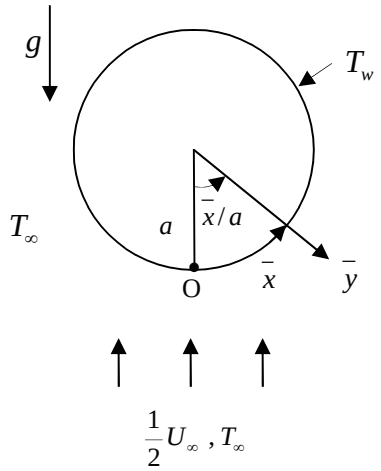

Fig. 1. Physical model and coordinate system.

we assume that the velocity of the free stream is $(1/2)\,U_\infty$. Under these assumptions along with the Boussinesq approximation, the boundary layer equations can be written as follows, see Garg and Rajagopal [12] and Mushtaq et al. [18],

Continuity equation

$$\frac{\partial \bar{u}}{\partial \bar{x}} + \frac{\partial \bar{v}}{\partial \bar{y}} = 0 \tag{1}$$

Momentum equation

$$\bar{u}\frac{\partial \bar{u}}{\partial \bar{x}} + \bar{v}\frac{\partial \bar{u}}{\partial \bar{x}} = \bar{u}_e \frac{d\bar{u}_e}{d\bar{x}} + \upsilon \frac{\partial^2 \bar{u}}{\partial \bar{y}^2} + \frac{k_0}{\rho}\left[\frac{\partial}{\partial \bar{x}}\left(\bar{u}\frac{\partial^2 \bar{u}}{\partial \bar{y}^2}\right) + \bar{v}\frac{\partial^3 \bar{u}}{\partial \bar{y}^3} + \frac{\partial \bar{u}}{\partial \bar{y}}\frac{\partial^2 \bar{v}}{\partial \bar{y}^2}\right] + g\,\beta\,(T - T_\infty)\sin(\bar{x}/a) \tag{2}$$

Energy equation

$$\bar{u}\frac{\partial T}{\partial \bar{x}} + \bar{v}\frac{\partial T}{\partial \bar{y}} = \alpha \frac{\partial^2 T}{\partial \bar{y}^2} \tag{3}$$

subject to the boundary conditions

$$\begin{aligned} &\bar{u} = \bar{v} = 0, \quad T = T_w \quad \text{at} \quad \bar{y} = 0, \quad \bar{x} \geq 0 \\ &\bar{u} = \bar{u}_e(x), \quad \partial \bar{u}/\partial \bar{y} = 0, \quad T = T_\infty \quad y \to \infty, \quad \bar{x} \geq 0 \end{aligned} \tag{4}$$

where $\bar{x}$ and $\bar{y}$ are the Cartesian coordinates measured along the surface of the cylinder starting from the lower stagnation point of the cylinder and $\bar{y}$ is the coordinate measured normal to the surface of the cylinder, $\bar{u}$ and $\bar{v}$ are the velocity components along the $\bar{x}-$ and $\bar{y}-$axes, $\bar{u}_e(\bar{x})$ is the velocity outside the boundary layer, T is the fluid temperature, g is the acceleration due to gravity k_0 is the viscoelasticity and α, β, μ and ρ are the thermal diffusivity, thermal expansion coefficient, dynamic viscosity and density of the viscoelastic fluid.

We introduce now the following non-dimensional variables

$$\begin{aligned} x = \bar{x}/a, \quad y = \mathrm{Re}^{1/2}(\bar{y}/a), \quad u = \bar{u}/U_\infty, \quad v = \mathrm{Re}^{1/2}(\bar{v}/U_\infty) \\ u_e(x) = \bar{u}_e(\bar{x})/U_\infty, \quad \theta = (T - T_\infty)/(T_w - T_\infty) \end{aligned} \tag{5}$$

where Re = $U_\infty a/\nu$ is the Reynolds number. Substituting (5) into Eqs. (1) – (3), we get the following non-dimensional equations

$$\frac{\partial u}{\partial x}+\frac{\partial v}{\partial y}=0 \tag{6}$$

$$u\frac{\partial u}{\partial x}+v\frac{\partial u}{\partial y}=u_e\frac{d\,u_e}{d\,x}+\frac{\partial^2 u}{\partial y^2}+K\left[\frac{\partial}{\partial x}\left(u\frac{\partial^2 u}{\partial y^2}\right)+v\frac{\partial^3 u}{\partial y^3}+\frac{\partial u}{\partial y}\frac{\partial^2 v}{\partial y^2}\right]+\lambda\theta\sin x \tag{7}$$

$$u\frac{\partial T}{\partial x}+v\frac{\partial \theta}{\partial y}=\frac{1}{\mathrm{Pr}}\frac{\partial^2 \theta}{\partial y^2} \tag{8}$$

subject to the boundary conditions (4), which become

$$\begin{aligned} &u=v=0,\quad \theta=1 \quad \text{at} \quad y=0,\quad x\geq 0\\ &u=u_e(x),\quad \frac{\partial u}{\partial y}=0,\quad \theta=0 \quad \text{as} \quad y\to\infty,\quad x\geq 0 \end{aligned} \tag{9}$$

where Pr is the Prandtl number, K is the viscoelastic parameter and λ is the mixed convection parameter, which are defined as

$$K=\frac{k_0 U_\infty}{a\,\mu},\quad \lambda=\frac{\mathrm{Gr}}{\mathrm{Re}^2} \tag{10}$$

with $Gr=g\,\beta\,(T_w-T_\infty)\,a^3/\upsilon^2$ being the Grashof number. It should be mentioned that $\lambda>0$ corresponds to assisting flow (heated cylinder), $\lambda<0$ corresponds to opposing flow (cooled cylinder) and $\lambda=0$ corresponds to the forced convection flow, respectively.

3. Solution

To solve Eqs. (6)-(8) with the boundary conditions (9), we follow Merkin [20] and assume that $u_e(x)=\sin x$. Thus, we look for a solution of these equations of the following form

$$\psi=x\,f(x,y),\quad \theta=\theta(x,y) \tag{11}$$

where ψ is the stream function defined as $u=\partial\psi/\partial y$ and $v=-\partial\psi/\partial x$. Substituting (11) into Eqs. (7) and (8), we obtain

$$\begin{aligned} &\frac{\partial^3 f}{\partial y^3}+f\frac{\partial^2 f}{\partial y^2}-\left(\frac{\partial f}{\partial y}\right)^2+\frac{\sin x\cos x}{x}+\lambda\,\frac{\sin x}{x}\,\theta+K\left\{2\frac{\partial f}{\partial y}\frac{\partial^3 f}{\partial y^3}-f\frac{\partial^4 f}{\partial y^4}-\left(\frac{\partial^2 f}{\partial y^2}\right)^2\right.\\ &\left.+x\left(\frac{\partial^2 f}{\partial x\partial y}\frac{\partial^3 f}{\partial y^3}-\frac{\partial f}{\partial x}\frac{\partial^4 f}{\partial y^4}+\frac{\partial f}{\partial y}\frac{\partial^4 f}{\partial x\partial y^3}-\frac{\partial^2 f}{\partial y^2}\frac{\partial^3 f}{\partial x\partial y^2}\right)\right\}=x\left(\frac{\partial f}{\partial y}\frac{\partial^2 f}{\partial x\partial y}-\frac{\partial f}{\partial x}\frac{\partial^2 f}{\partial y^2}\right) \end{aligned} \tag{12}$$

$$\frac{1}{\Pr}\frac{\partial^2\theta}{\partial y^2}+f\frac{\partial\theta}{\partial y}=x\left(\frac{\partial f}{\partial y}\frac{\partial\theta}{\partial x}-\frac{\partial f}{\partial x}\frac{\partial\theta}{\partial y}\right) \tag{13}$$

subject to the boundary conditions

$$\begin{aligned} &f=\frac{\partial f}{\partial y}=0,\quad \theta=1 \quad \text{at} \quad y=0,\quad x\geq 0\\ &\frac{\partial f}{\partial y}=\frac{\sin x}{x},\quad \frac{\partial^2 f}{\partial y^2}=0,\quad \theta=0 \quad \text{as} \quad y\to\infty,\quad x\geq 0 \end{aligned} \tag{14}$$

It is worth mentioning that when $K=0$, Eqs. (12) and (13) reduce to the equations governing the mixed convection boundary layer flow of a viscous and incompressible (Newtonian)) fluid studied by Merkin [20].

At the lower stagnation point of the cylinder, $x\approx 0$, Eqs. (12) and (13) reduce to the following ordinary differential equations

$$f'''+f\,f''-f'^2+1+\lambda\theta+K\left(2f'f'''-ff^{iv}-f''^2\right)=0 \tag{15}$$

$$\frac{1}{\Pr}\theta''+f\,\theta'=0 \tag{16}$$

with the boundary conditions

$$\begin{aligned} &f(0)=f'(0)=0,\quad \theta(0)=1\\ &f'(\infty)=1,\quad f''(\infty)=0,\quad \theta(\infty)=0 \end{aligned} \tag{17}$$

where primes denote the differentiation with respect to y.

The physical quantities of principal interest in this problem are the skin friction coefficient C_f and heat transfer coefficient Q_w. We define these coefficients in non-dimensional form as

$$C_f=\mathrm{Re}^{1/2}\frac{\tau_w}{\rho U_\infty^2},\quad Q_w=\mathrm{Re}^{-1/2}\frac{a\,q_w}{k(T_w-T_\infty)} \tag{18}$$

where τ_w and q_w are the skin friction and heat flux from the surface of the cylinder, which are given by

$$\tau_w=\mu\left(\frac{\partial\bar{u}}{\partial\bar{y}}\right)_{\bar{y}=0}+k_0\left(\bar{u}\,\frac{\partial^2\bar{u}}{\partial\bar{x}\partial\bar{y}}+\bar{v}\,\frac{\partial^2\bar{u}}{\partial\bar{y}^2}+2\frac{\partial\bar{u}}{\partial\bar{x}}\frac{\partial\bar{u}}{\partial\bar{y}}\right)_{\bar{y}=0}\qquad q_w=-k\left(\frac{\partial T}{\partial\bar{y}}\right)_{y=0} \tag{19}$$

k being the thermal conductivity of the viscoelastic fluid. Using (5) and (11), we obtain

$$C_f = x\left(\frac{\partial^2 f}{\partial y^2}\right)_{y=0}, \quad Q_w = -\left(\frac{\partial \theta}{\partial y}\right)_{y=0} \tag{20}$$

For small values of the viscoelastic parameter K ($<<1$), we look for a solution of Eqs. (15) and (16) subject to the boundary conditions (17) in series of the form

$$\begin{aligned} f(y) &= f_0(y) + K\, f_1(y) + K^2\, f_2(y) + \ldots \\ \theta(y) &= \theta_0(y) + K\,\theta_1(y) + K^2\,\theta_2(y) + \ldots \end{aligned} \tag{21}$$

where the functions $f_i(y)$ and $\theta_i(y)$ ($i = 0,1,2$) are given by the following three sets of equations with the corresponding boundary conditions

$$\begin{aligned} & f_0''' + f_0\, f_0'' - f_0'^2 + 1 + \lambda\,\theta_0 = 0 \\ & \frac{1}{\mathrm{Pr}}\theta_0'' + f_0\,\theta_0' = 0 \\ & f_0(0) = f_0'(0) = 0, \quad \theta_0(0) = 1 \\ & f_0'(\infty) = 1, \quad \theta_0(\infty) = 0; \end{aligned} \tag{22}$$

$$\begin{aligned} & f_1''' + f_0\, f_1'' - 2\, f_0'\, f_1' + f_0''\, f_1 + \lambda\,\theta_1 = f_0\, f_0'''' - 2\, f_0'\, f_0''' + f_0''^2 \\ & \frac{1}{\mathrm{Pr}}\theta_1'' + f_0\,\theta_1' = -f_1\,\theta_0' \\ & f_1(0) = f_1'(0) = 0, \quad \theta_1(0) = 0 \\ & f_1'(\infty) = 0, \quad \theta_1(\infty) = 0; \end{aligned} \tag{23}$$

$$\begin{aligned} & f_2''' + f_0 f_2'' - 2\, f_0'\, f_2' + f_0''\, f_2 + \lambda\,\theta_2 = f_1'^2 - f_1\, f_1'' + f_0\, f_1'''' + f_1\, f_0'''' \\ & \qquad\qquad - 2\,(f_0'\, f_1''' + f_1'\, f_0''') + 2\, f_0''\, f_1'' \\ & \frac{1}{\mathrm{Pr}}\theta_2'' + f_0\,\theta_2' = -f_1\,\theta_1' - f_2\,\theta_0' \\ & f_2(0) = f_2'(0) = 0, \quad \theta_2(0) = 0 \\ & f_2'(\infty) = 0, \quad \theta_2(\infty) = 0 \end{aligned} \tag{24}$$

Thus, the reduced skin friction and heat transfer from the surface of the cylinder are given by

$$\begin{aligned} f''(0) &= f_0''(0) + f_1''(0)\, K + f_2''(0)\, K^2 + \ldots \\ -\theta'(0) &= \theta_0'(0) + \theta_1'(0)\, K + \theta_2'(0)\, K^2 + \ldots \end{aligned} \tag{25}$$

for $K << 1$.

4. Results and discussion

The systems of equations (12-14) and (22-24) were solved numerically for some values of the mixed convection parameter λ and viscoelastic parameter K using the Keller-box method, which is described in the book by Cebeci and Bradshaw [19]. All three cases of the assisting ($\lambda > 0$) flow, opposing ($\lambda < 0$) flow and forced convection flow ($\lambda = 0$) are considered. In order to save space we present here results only the case when the Prandtl number Pr is one. The value of $\eta = \eta_\infty = 10$ at infinity with the step size of $\Delta\eta = 0.02$ and $\Delta x = 0.02$ has been used for the computation. The iterations were continued until an accuracy of 10^{-6} was achieved.

The comparison of the present results for the skin friction coefficient C_f and the heat transfer from the cylinder Q_w with those of Merkin [20] and Nazar *et al*. [21] for a Newtonian fluid ($K = 0$) is shown in Figs. 2 and 3. The comparison shows that the numerical solutions obtained by the present authors are in very good agreement with those of Merkin [20] and Nazar *et al*. [21]. We are, therefore, confident that the present results are very accurate. The trend exhibited by the curves is consistent with the expected effect of favourable pressure gradient. A positive mixed convection or buoyancy force parameter ($\lambda > 0$) induces a favourable pressure gradient that enhances the fluid motion, which in turn increases the skin friction coefficient C_f and hence the local heat transfer coefficient Q_w also increases and the heat transfer from the cylinder is increased with λ (see Fig. 3).

The variation of C_f and Q_w with x for a viscoelastic fluid ($K > 0$) is shown in Figs. 4 to 7 at different positions x at the surface of the cylinder and some values of λ when $K = 0.2$ and 1 and $\mathrm{Pr} = 1$. Numerical values of C_f and Q_w are also given in Tables 1 to 4. It is found that both skin friction C_f and heat transfer Q_w coefficients decrease as K is increased. A similar trend has been observed by Gard and Rajagopal [12] for the problem of forced convection flow of a viscoelastic fluid past a wedge and by Kumari *et al.* [1] for the problem of mixed convection flow of a viscoelastic fluid past a vertical wedge. This can be attributed to the thickening of momentum and thermal boundary layers as K increases. Kumari *et al*. [1] have explained that the increase in the boundary layer thickness with K can be attributed to tensile stress in the boundary layer, which cause an axial contraction and hence the thickening of the boundary layer in the transverse direction. We can also see from Figs. 4 to 7 and tables 1 to 4 that, as it is expected, the boundary-layer separates from the cylinder for some negative values of λ (cooling cylinder) and also for some positive values of λ (heated cylinder). On the other hand, the results show that, as for the case of a Newtonian fluid, increasing λ delays separation of the

boundary layer from the cylinder and that separation can be suppressed completely in the range $0 \le x \le \pi$ for sufficiently large values of $\lambda > 0$. In addition, Figs. 4 to 7 and Tables 1 to 4 show that there is a value of $\lambda = \lambda_c(K)$, which depends on K, below which a boundary layer solution is not possible. As it was explained by Merkin [20] for the case of a Newtonian fluid ($K = 0$), the reason is that for $\lambda < 0$ the cylinder is cooled and the natural convection boundary layer would start at the top stagnation point of the cylinder ($x = \pi$) and for sufficiently small λ there comes a point where the flow of the stream upwards cannot overcome the tendency of the fluid next to the cylinder to move downwards under the action of the buoyancy forces.

Using the boundary conditions (14) and the fact that $(\partial^2 f / \partial y^2)_{y=0} = 0$ at $x = x_s$, we get from Eq. (12), see Merkin [20],

$$x_s \left(\frac{\partial^3 f}{\partial y^3} \right)_{y=0} + (\lambda + \cos x) \sin x = 0 \tag{26}$$

Though $(\partial^2 f / \partial y^2)_{y=0} = 0$ at $x = x_s$, the streamwise velocity component $\partial f / \partial y > 0$ near $y = 0$ and so $\left(\partial^3 f / \partial y^3\right)_{y=0} \ge 0$ at $x = x_s$. From (26) it means that $(\lambda + \cos x)\sin x \le 0$, which cannot hold in $0 \le x \le 180^0$ for $\lambda > 1$ and any value of $K\,(> 0)$.

The numerical solutions indicate that the value of $\lambda_c(K)$ which first gives no separation lies in the ranges $0.88 < \lambda_c < 0.89$ for $K = 0$ (Newtonian fluid), $5.76 < \lambda_c < 5.77$ for $K = 0.2$ and $5.08 < \lambda_c < 5.09$ for $K = 1$, respectively. We notice that the value of $\lambda_c(K)$ decreases with the increase of K. Thus, for a viscoelastic fluid ($K > 0$), the value of $\lambda_c(K)$ for which separation of the boundary first takes place is much lower than for a Newtonian fluid ($K = 0$). In other words, the separation of the boundary layer for a viscoelastic fluid is less delayed in comparison with that of a Newtonian fluid.

The variation of the boundary layer separation point x_s with λ is shown in Figs. 8 for $K = 0$ (Newtonian fluid), $K = 0.2$ and $K = 1$ when $\Pr = 1$. It can be seen from this figure that $\lambda_c(K)$ increases with increase in the value of K.

Further, Table 5 presents some values of the reduced skin friction $f''(0)$ and heat flux at the surface of the cylinder $-\theta'(0)$ given by the series (25) for small values of the viscoelastic parameter K ($<<1$) without using the extra boundary condition $f''(\infty) = 0$. The values obtained by direct numerical integration of Eqs. (15) and (16) using the boundary conditions (17) with the extra boundary condition $f''(\infty) = 0$ are also included in Table 5. The classical results reported by Hiemenz [22] and Eckert [23]

for $K = 0$ (Newtonian fluid) and $\lambda = 0$ (forced convection flow) are also included in this Table. In addition, the results reported by Ariel [14] for a viscoelastic fluid ($K > 0$) obtained using the direct numerical solution of Eqs. (15) and (16) with the boundary conditions (17) when $\lambda = 0$ (forced convection flow) and the series solutions for small values of K ($<<1$) are included in Table 5. In all cases he results are found to be in very good agreement. Further, it is noticed that the results based on the series expansion agree well with the exact numerical solution of Eqs. (15) and (16). Therefore, the advantage of using the extra boundary condition $f''(\infty) = 0$ over the series expansion is that the analysis is valid even for large values of the parameter K. Garg and Rajagopal [11] have shown that significant deviations from the Newtonian behaviour are possible for even moderately large values of K.

Finally, Figs. 9 and 10 illustrate the velocity and temperature profiles at the lower stagnation point of the cylinder against y for several values of the parameter K when $\lambda = 1$ (assisting flow) and $\lambda = -1$ (opposing flow), respectively, and $\Pr = 1$. These figures show how the viscoelastic parameter K affects the fluid velocity and temperature profiles. Thus, Figs. 9 show that the velocity profiles decrease when K is increased and that the values of these profiles are lower for a viscoelastic fluid than for a Newtonian fluid ($K = 0$). Therefore, the thickness of the velocity boundary layer for a viscoelastic fluid is higher than for a Newtonian fluid. Further, it is seen from Figs. 7 that the velocity profiles are lower for the case of the assisting flow ($\lambda = 1$) than those for an opposing flow ($\lambda = -1$), respectively. The reverse trend is observed for the temperature profiles, which are shown in Fig. 10.

5. Conclusion

The steady mixed convection boundary layer flow of an incompressible viscoelastif fluid past an isothermal horizontal circular cylinder has been investigated numerically. The governing boundary layer equations are transformed into a non-dimensional form and the resulting nonlinear system of partial differential equations is solved numerically using the Keller-box method. Both the cases when the mixed convection parameter $\lambda > 0$ ($T_w > T_\infty$) heated cylinder and $\lambda < 0$ ($T_w < T_\infty$) cooled cylinder are considered. It is found that for a heated cylinder ($\lambda > 0$) the separation of the boundary layer is delayed and that there is a value of $\lambda = \lambda_c(K)$ for which the boundary layer does not separate at all. The value of $\lambda_c(K)$ increases with the increase of the viscoelastic parameter K. On the other hand, for a cooler cylinder ($\lambda < 0$), the buoyancy forces also retard the fluid and therefore the separation point is brought nearer to the lower stagnation point. A value of $\lambda = \lambda_s(K)$ (< 0) has been found for which the boundary layer separates at this point. It is found that this value of $\lambda_s(K)$ decreases as the parameter K increases.

For values of $\lambda < \lambda_s(K)$ a boundary layer solution of Eqs. (12) and (13) subject to the boundary conditions (14) is not possible. The results of Merkin [20] for viscous fluids can be recovered easily when the viscoelastic parameter $K = 0$.

Aknowledgements

The authors wish to express their thanks to the reviewers for the valuable comments and suggestions.

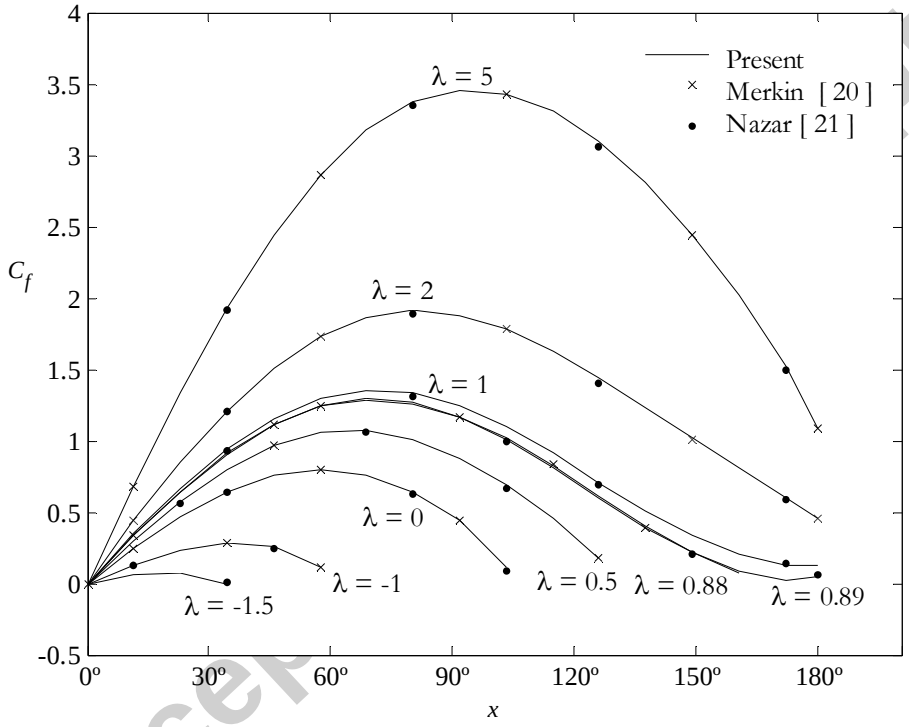

Fig. 2. Comparison of the local skin friction C_f for $K = 0$ (Newtonian fluid), Pr = 1 and various values of λ.

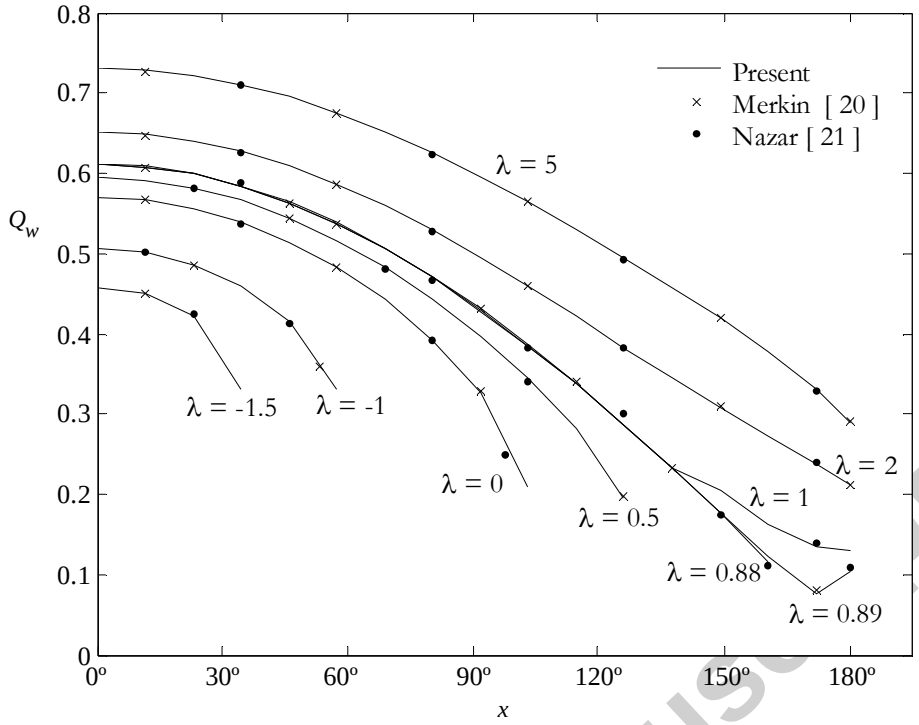

Fig. 3. Comparison of the heat transfer coefficient Q_w for $K = 0$ (Newtonian fluid), Pr = 1 and various values of λ.

Table 1. Values of the local skin friction coefficient C_f for $K = 0.2$, Pr = 1 and various values of λ.

x	λ										
	-1.7	-1.2	-1	-0.2	0	1	5.76	5.77	6	8	10
0º	0.000000	0.000000	0.000000	0.000000	0.000000	0.000000	0.000000	0.000000	0.000000	0.000000	0.000000
10º	0.007813	0.075842	0.095065	0.169066	0.188567	0.261702	0.486962	0.515861	0.474144	0.614049	0.694980
20º		0.137463	0.181342	0.327172	0.365709	0.512363	1.010971	1.020135	1.041244	1.215724	1.376883
30º		0.169083	0.238510	0.463727	0.520436	0.741418	1.466470	1.501591	1.533050	1.792980	2.032944
40º			0.257160	0.562992	0.624907	0.908811	1.933590	1.949691	1.991247	2.334419	2.651017
50º				0.630664	0.713081	1.074251	2.318635	2.354904	2.406207	2.829577	3.219836
60º				0.650538	0.753463	1.194724	2.689959	2.676071	2.735755	3.227941	3.681247
70º					0.739873	1.265578	2.973755	2.978261	3.074396	3.610686	4.129578
80º						1.284609	3.221288	3.217793	3.294293	3.924041	4.502841
90º							3.384216	3.390985	3.474664	4.162894	4.794822
100º							-	3.495771	3.585573	4.323578	5.000657

Table 2. Values of the local heat transfer coefficient Q_w for $K = 0.2$, Pr = 1 and various values of λ.

x	λ										
	-1.7	-1.2	-1	-0.2	0	1	5.76	5.77	6	8	10
0º	0.412206	0.473390	0.489810	0.538464	0.548077	0.587800	0.699263	0.699432	0.703288	0.733679	0.759703
10º	0.402968	0.469605	0.486704	0.536168	0.545829	0.585939	0.698097	0.698126	0.702238	0.732440	0.758508
20º		0.457817	0.476582	0.529237	0.539012	0.580321	0.694121	0.694206	0.698099	0.728737	0.754924
30º		0.437275	0.459559	0.517571	0.527573	0.570973	0.687364	0.687711	0.691649	0.722593	0.748980
40º			0.433531	0.502232	0.514416	0.560355	0.678861	0.678697	0.682698	0.714061	0.740720
50º				0.480697	0.494088	0.544255	0.668180	0.667245	0.671325	0.703209	0.730204
60º				0.453277	0.468461	0.524541	0.654015	0.654937	0.659099	0.691531	0.718873
70º					0.436886	0.501286	0.639052	0.639146	0.641727	0.676521	0.704287
80º						0.474589	0.620440	0.621264	0.625642	0.659477	0.687687
90º							0.601702	0.601440	0.605935	0.640515	0.669168
100º								0.579831	0.584442	0.619747	0.648816

Table 3. Values of the local skin friction coefficient C_f for $K = 1$, Pr = 1 and various values of λ.

x	λ										
	-1.5	-1.2	-1	-0.5	0	1	5.08	5.09	6	8	10
0º	0.000000	0.000000	0.000000	0.000000	0.000000	0.000000	0.000000	0.000000	0.000000	0.000000	0.000000
10º	0.019289	0.052169	0.069744	0.103117	0.134492	0.173422	0.333750	0.321618	0.353994	0.398644	0.454355
20º	0.022726	0.093682	0.129311	0.199976	0.256058	0.341456	0.631982	0.637747	0.689319	0.791393	0.877552
30º		0.117588	0.173691	0.284381	0.373377	0.509827	0.920633	0.943049	1.013946	0.791393	1.313246
40º		0.108808	0.194033	0.346535	0.468475	0.663637	1.222005	1.232478	1.322962	0.791393	1.707582
50º			0.177420	0.389534	0.547616	0.785869	1.501428	1.501417	1.611837	1.878135	2.101442
60º			-	0.401773	0.597900	0.889338	1.732533	1.722555	1.886163	2.142536	2.446388
70º					0.620877	0.976946	1.957941	1.941830	2.122024	2.476852	2.761005
80º					0.611955	1.030342	2.134117	2.130549	2.327203	2.687289	3.057205
90º						1.063992	2.281085	2.286574	2.499462	2.938649	3.311983
100º								2.408461	2.637173	3.085509	3.511960

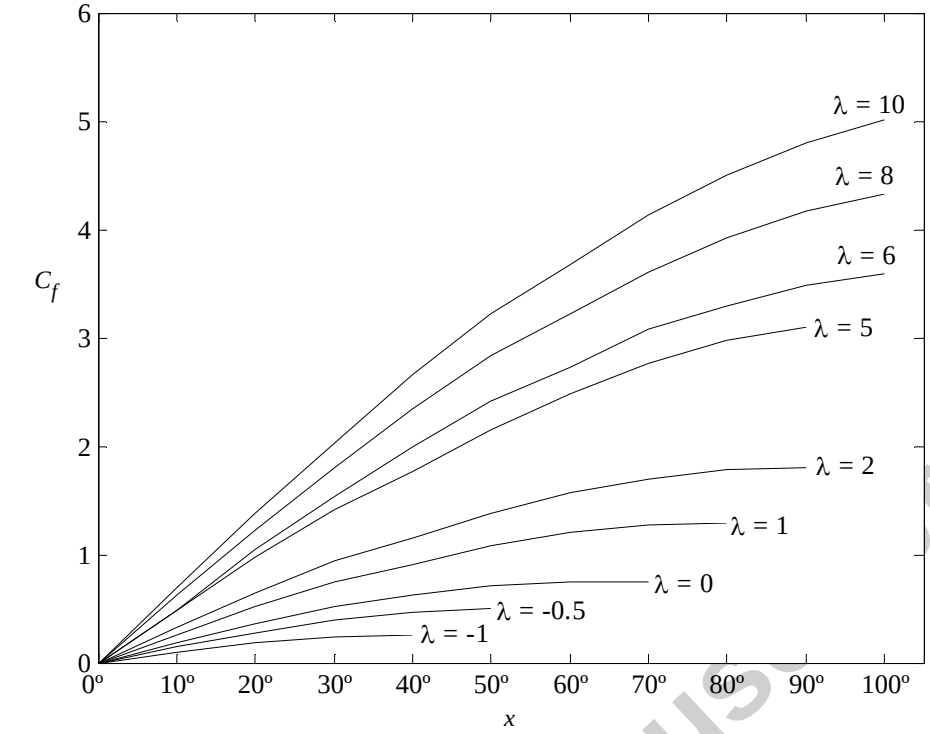

Fig. 4. Variation of the local skin friction coefficient C_f for $K = 0.2$, Pr = 1 and various values of λ.

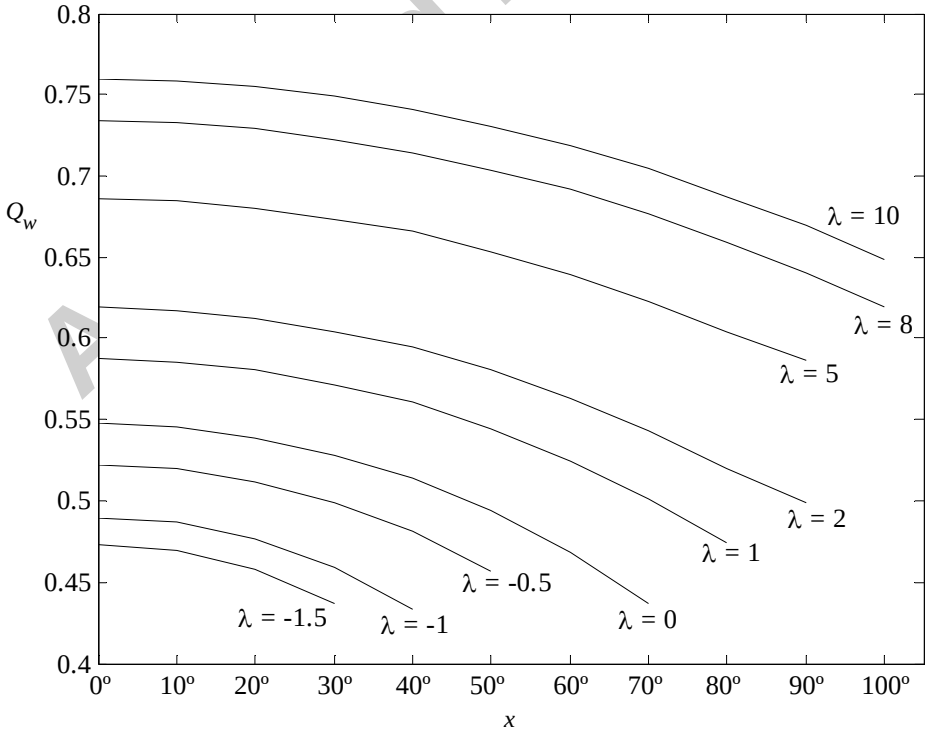

Fig. 5. Variation of the local heat transfer coefficient Q_w for $K = 0.2$, Pr = 1 and various values of λ.

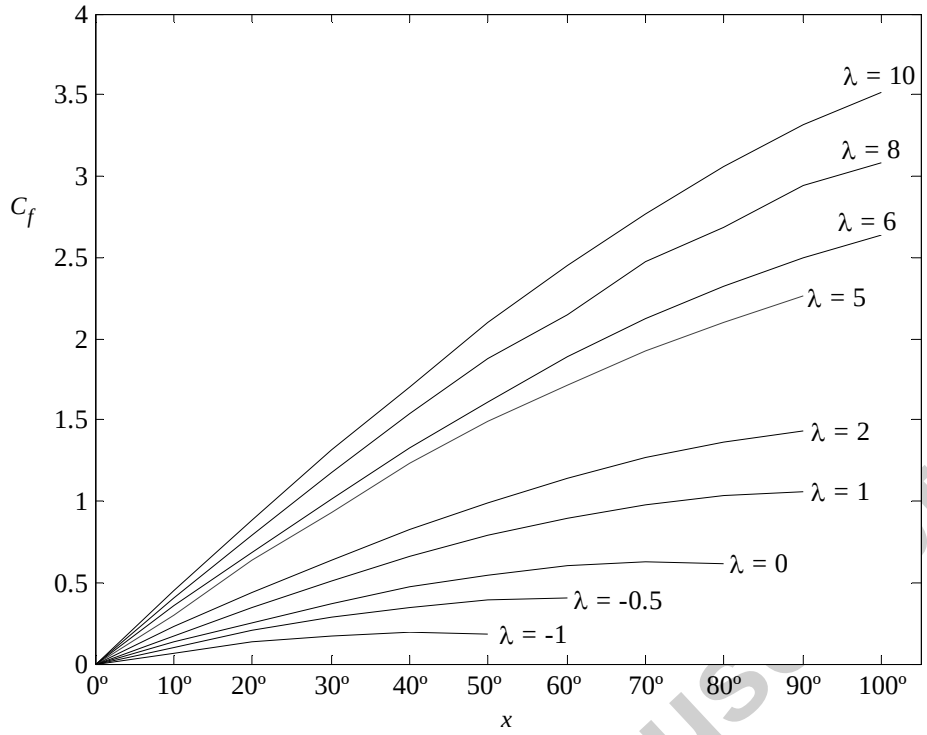

Fig. 6. Variation of the local skin friction coefficient C_f for $K = 1$, Pr = 1 and various values of λ.

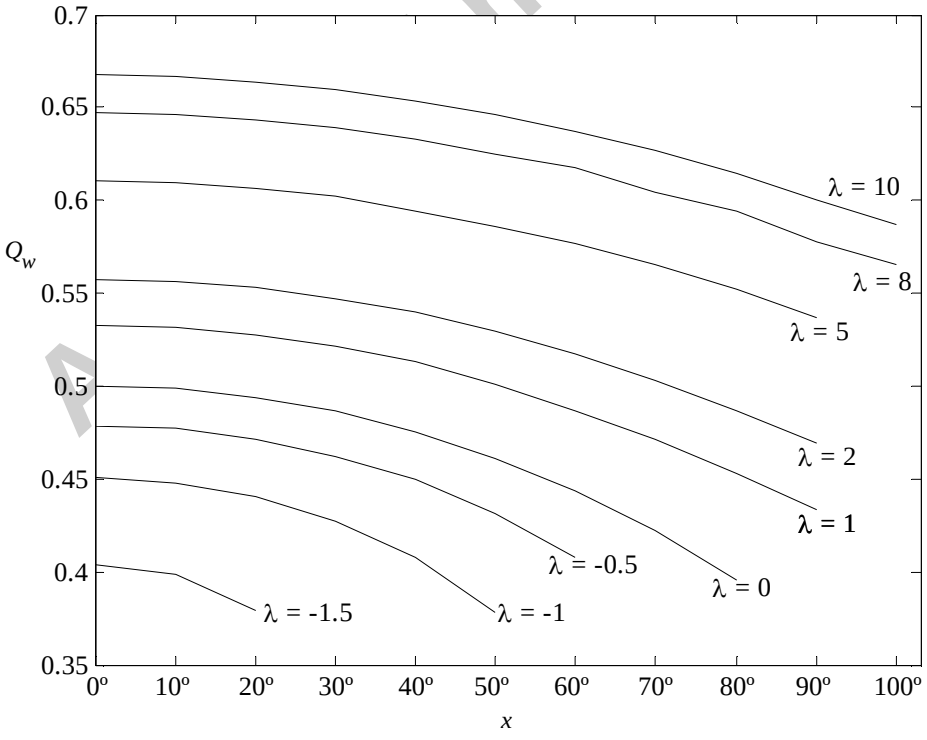

Fig. 7. Variation of the local heat transfer coefficient Q_w for $K = 1$, Pr = 1 and various values of λ.

Table 4. Values of the local heat transfer coefficient C_f for $K = 1$, Pr = 1 and various values of λ.

x	λ										
	-1.5	-1.2	-1	-0.5	0	1	5.08	5.09	6	8	10
0º	0.403657	0.435250	0.450362	0.478927	0.500411	0.533005	0.611397	0.611539	0.623797	0.647291	0.667322
10º	0.398706	0.432235	0.447818	0.477076	0.498772	0.531797	0.610347	0.610566	0.622811	0.646396	0.666414
20º	0.379615	0.423299	0.440389	0.471472	0.494198	0.527670	0.607568	0.607647	0.620005	0.643694	0.663890
30º		0.406303	0.427511	0.461985	0.486116	0.521390	0.602534	0.602808	0.615401	0.643694	0.659477
40º		0.379684	0.407854	0.449397	0.475361	0.512723	0.595474	0.596092	0.609036	0.643694	0.653694
50º			0.377859	0.431466	0.460556	0.500467	0.587355	0.587558	0.600965	0.625078	0.645909
60º			-	0.408077	0.443178	0.486895	0.577682	0.578386	0.590849	0.617239	0.637040
70º					0.422237	0.471064	0.565340	0.566621	0.579524	0.604450	0.626760
80º					0.395685	0.453044	0.552672	0.553304	0.566740	0.594088	0.614413
90º						0.432927	0.537272	0.538557	0.552605	0.577981	0.600648
100º								0.522515	0.537234	0.565413	0.586427

Table 5. Values of $f''(0)$ and $-\theta'(0)$ for various values of K when $\lambda = 0, 1$ and -1 for $\mathrm{Pr} = 1$.

K	λ = 0				λ = 1				λ = –1			
	Series		Numerical		Series		Numerical		Series		Numerical	
	$f''(0)$	$-\theta'(0)$	$f''(0)$	$-\theta'(0)$	$f''(0)$	$-\theta'(0)$	$f''(0)$	$-\theta'(0)$	$f''(0)$	$-\theta'(0)$	$f''(0)$	$-\theta'(0)$
0			1.232632 1.232588*	0.570519 0.5700**			1.736738	0.615601			0.651118	0.509534
0.01	1.222693	0.569511	1.221447	0.569130	1.718360	0.614079	1.718552	0.613861	0.649610	0.509081	0.643624	0.505705
0.1	1.135982 1.137088‡	0.556038	1.134172 1.134114‡	0.558175	1.558738	0.591337	1.580229	0.600089	0.621103	0.503818	0.601190	0.497588
0.2	1.045412 1.078392‡	0.531793	1.058180 1.058131‡	0.548077	1.393405	0.546974	1.464141	0.587800	0.589979	0.495482	0.562568	0.489810
0.3	0.960922	0.497784	0.996886	0.539500	1.240729	0.482513	1.372892	0.577594	0.559437	0.484524	0.530390	0.483012
0.4	0.882512	0.454010	0.945907	0.532036	1.100711	0.397954	1.298364	0.568851	0.529474	0.470946	0.502993	0.476970
0.5	0.810182	0.400472	0.902535	0.525424	0.973349	0.293296	1.235808	0.561198	0.500093	0.454747	0.479271	0.471533
0.6	0.743933	0.337171	0.864985	0.519487	0.858645	0.168540	1.182212	0.554389	0.471291	0.435927	0.458452	0.466588
0.7	0.683763	0.264105	0.832019	0.514101	0.756598	0.023685	1.135550	0.548256	0.443071	0.414486	0.439978	0.462056
0.8	0.629673	0.181274	0.802749	0.509171	0.666997	-0.141268	1.094396	0.542677	0.415431	0.390425	0.423434	0.457872
0.9	0.581664	0.088680	0.776511	0.504626	0.590210	-0.326320	1.057711	0.537559	0.388372	0.363743	0.408500	0.453987
1			0.752803 0.752766‡	0.500411			1.024719	0.532833			0.394929	0.450362
2			0.596874 0.596769‡	0.469671			0.810695	0.498821			0.304357	0.423419
3			0.510914 0.510703‡	0.449922			0.694301	0.477261			0.254015	0.405786
4			0.454295 0.453968‡	0.435499			0.617991	0.461601			0.221003	0.392827
5			0.413321 0.412885‡	0.424228			0.562865	0.449394			0.197308	0.382679
8			0.336042 0.335335‡	0.400685			0.458930	0.423929			0.153389	0.361509
10			0.303669 0.302828‡	0.389777			0.415342	0.412127			0.135426	0.351747

*Hiemenz [22] ; **Eckert [23] ; ‡Ariel [14]

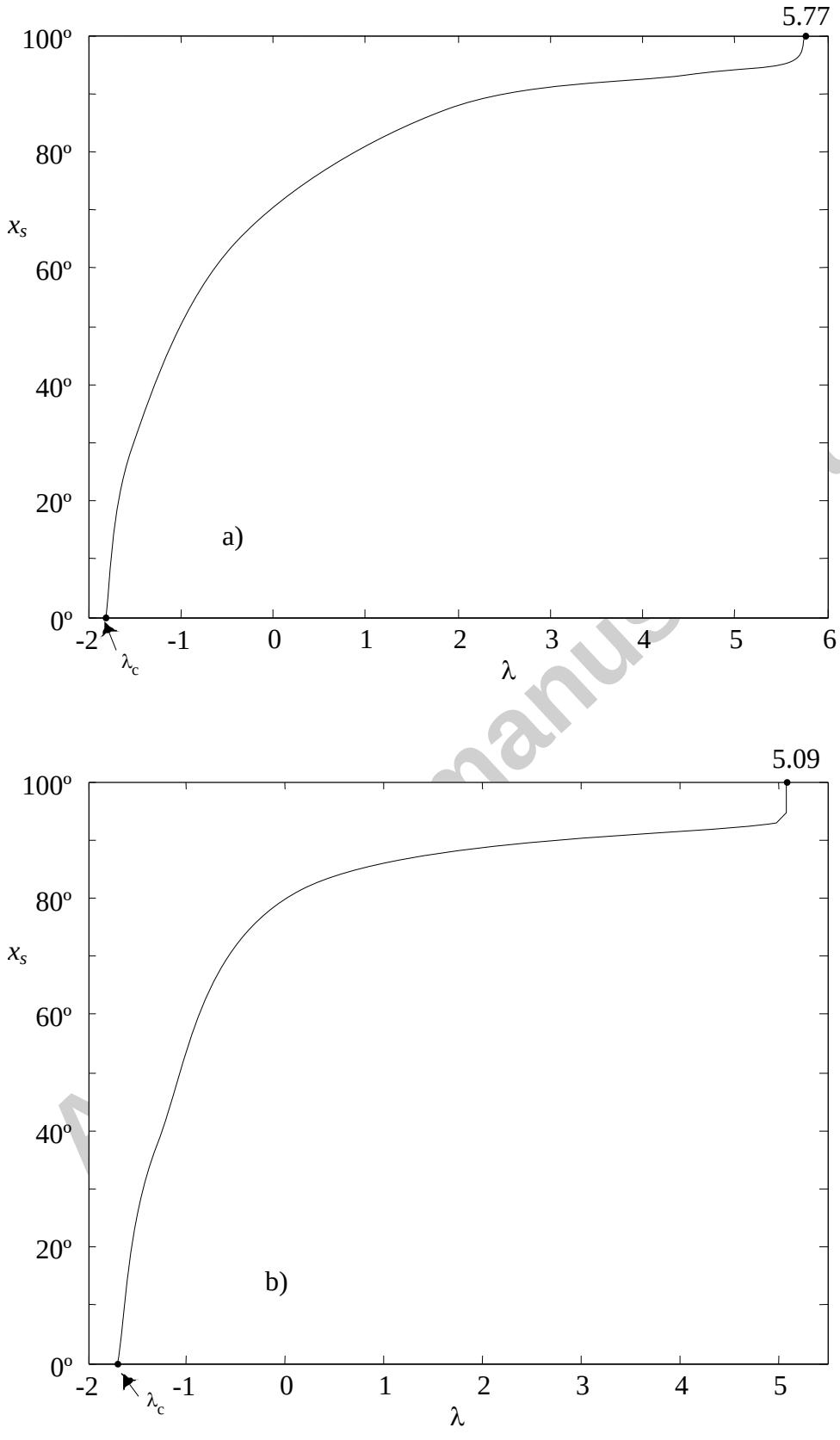

Fig. 8. Variation of the boundary layer separation point x_s with λ for

$\mathrm{Pr} = 1$: a) $K = 0.2$ and b) $K = 1$.

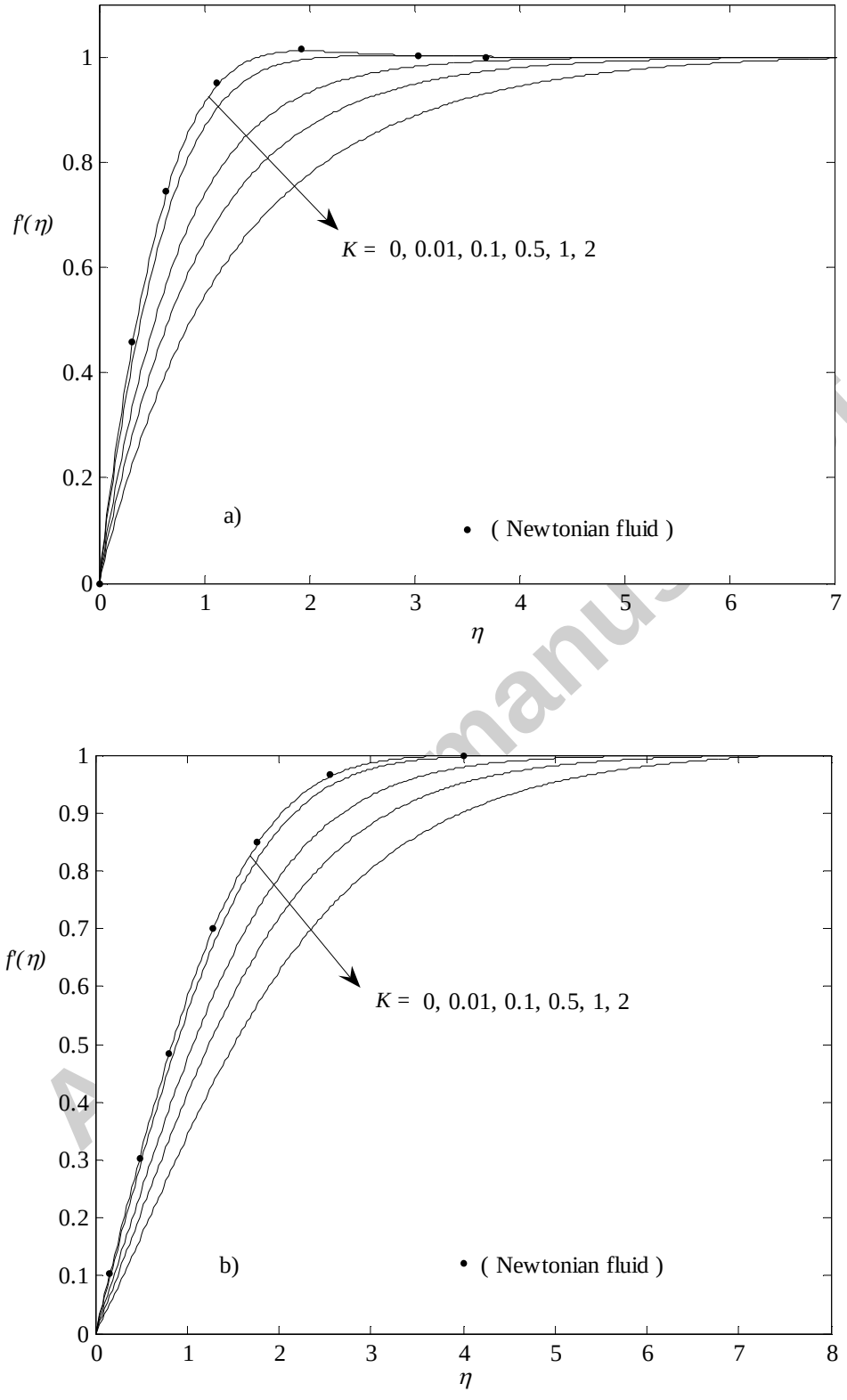

Fig. 9.Velocity profiles at the lower stagnation point for Pr = 1 and various value of K; a) $\lambda = 1$ (assisting flow) and b) $\lambda = -1$ (opposing flow).

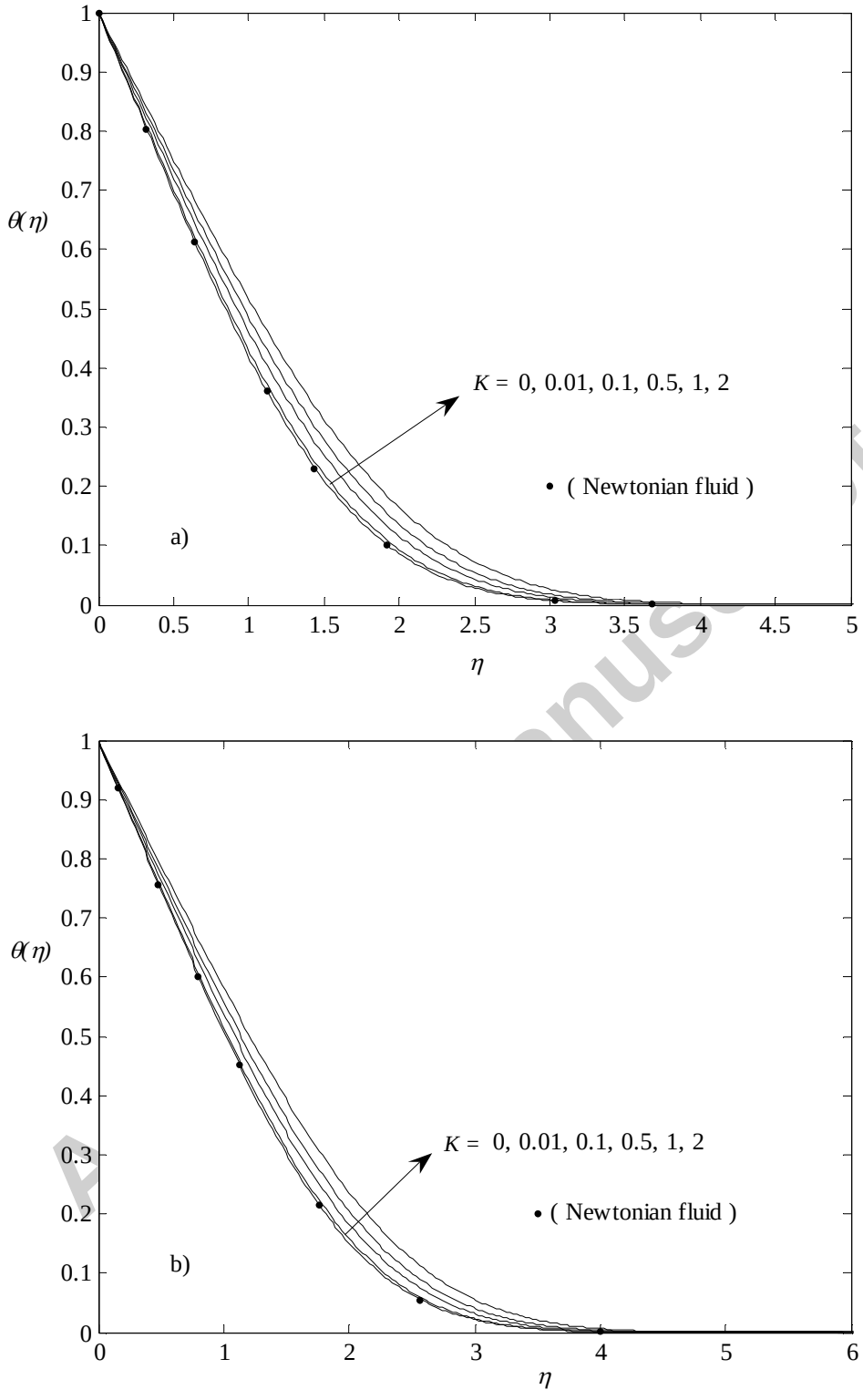

Fig. 10. Temperature profiles at the lower stagnation point for Pr = 1 and various value of K: a) $\lambda = 1$ (assisting flow) and b) $\lambda = -1$ (opposing flow).

References

[1] M. Kumari, H.S. Takhar, G. Nath, Nonsimilar mixed convection flow of a non-Newtonian fluid past a vertical wedge, Acta Mechanica 113 (1995) 205 - 213.

[2] R.S. Rivlin, J.L. Ericksen, Stress deformation relations for isotropic materials, J. Rational Mech. Anal. 4 (1955) 323 - 425.

[3] C. Truesdell, W. Noll, The Non-Linear Field Theories of Mechanics, 2nd edition, Springer, New York, 1992.

[4] M. Massoudi, Local non-similarity solutions for the flow of a non-Newtonian fluid over a wedge, Int. J. Non-Linear Mech. 36 (2001) 961-976.

[5] J.G. Oldroyd, On the formulation of rheological equations of state, Proc. Roy. Soc. London A 200 (1950) 523-541.

[6] D.W. Beard, K. Walters, Elastico-viscous boundary layer flows, Proc. Cambridge Philos. Soc. 60 (1964) 667-

[7] K.R. Rajagopal, T.Y. Na, A.S. Gupta, Flow of a viscoelastic fluid over a stretching sheet, Rheol. Acta 23 (1984) 213-215.

[8] K.R. Rajagopal, On boundary conditions for fluids of the differential type, in: A. Sequeira (ed.), navier-Stokes Equations and Related Non-Linear Problems, Plenum, New York, 1995, pp. 273-278.

[9] K.R. Rajagopal, On the creeping flow of the second grade fluid, J. Non-Newtonain Fluid Mech. 15 (1984) 239-246.

[10] K.R. Rajagopal, P.N. Kaloni, Some remarks on boundary conditions for fluids of the differential type. In: G.A.C. Graham, S.K. Lamik (eds.), Continuum Mechanics and its Applications, Hemisphere, New York, 1989, pp. 035-942.

[11] V.K. Garg and K.R. Rajagopal, Stagnation point flow of a non-Newtonian fluid, Mech. Res. Communic. 17 (1990) 415-421.

[12] V.K. Garg, K.R. Rajagopal, Flow of a non-Newtonian fluid past a wedge, Acta Mechanica 88 (1991) 113-123.

[13] G.K. Rajeswari, S.L. Rathna, Flow of a particular class of non-Newtonian visco-elastic and visco-inelastic fluids near a stagnation point, J. Appl. Math. Phys. (ZAMP) 13 (1962) 43-57.

[14] P.D. Ariel, On extra boundary condition in the stagnation point flow of a second grade fluid, Int. J. Engng. Sci 40 (2002) 145-162.

[15] V.K. Garg, Non-Newtonian flow over a wedge with suction, Int. J. Numer. Methods in Fluids 15 (1992) 37-49.

[16] R. Cortell, A note on flow and heat transfer of a viscoelastic fluid over a stretching sheet, Int. J. Non-Linear Mech. 41 (2006) 78-85.

[17] T. Hayat, M. Sajid, Analytic solution for axisymmetric flow and heat transfer of a second grade fluid past a stretching sheet, Int. J. Heat Mass Transfer 50 (2007) 75-84.

[18] M. Mushtaq, S. Asghar, M.A. Hossain, Mixed convection flow of second grade fluid along a vertical stretching flat surface with variable surface temperature, Heat Mass Transfer (in press).

[19] T. Cebeci, P. Bradshaw, Physical and Computational Aspects of Convective Heat Transfer, Springer, New York, 1984.

[20] J.H. Merkin, Mixed convection from a horizontal circular cylinder, Int. J. Heat Mass Transfer 20 (1977) 73-77.

[21] R. Nazar, N. Amin, I. Pop, Mixed convection boundary-layer flow from a horizontal circular cylinder in micropolar fluids: case of constant wall temperature, Int. J. Numer. Methods Heat & Fluid Flow 13 (2003) 96-109.

[22] K. Hiemenz, Die Grenzschicht an einem in den gleichfrmigen Flssigkeitsstrom eingetauchten geraden Kreiszylinder, Dingl. Polytech. Journal 32 (1911) 321–410.

[23] E.R.G. Eckert, Die Berechnung des Wrmeberganges in der laminaren Grenzschicht umstrmter Krper. VDI Forschungsheft (1942) 461.